



## On the use of the stepped isostress method in the prediction of creep behavior of polyamide 6

Tedjini Mohsein, Sedira Lakhdar, Guerira Belhi

*Laboratoire de Génie Mécanique (LGM), University of Biskra, Algeria*

*mohsein.tedjini@gmail.com*

*l.sedira@univ-biskra.dz, http://orcid.org/0000-0003-1735-2195*

*b.guerira@univ-biskra.dz*

Kamel Meftah

*Laboratoire de Génie Energétique et Matériaux (LGEM), University of Biskra, Algeria*

*University of Batna 2, Algeria*

*k.meftah@univ-batna2.dz, http://orcid.org/0000-0002-5671-602X*

**ABSTRACT.** The stepped isostress method (SSM) is an advanced technique which allows the prediction of the long-term behavior and enables the construction of creep master curves of materials with short-term experimental tests. However, the performance of this method is highly dependent on the numerical model and the time spent in data processing. In this paper, the effect of the extrapolation techniques on the creep curves trend is investigated using the SSM data of Polyamide test. Three extrapolation functions are used to offset the delay of the stress history: polynomial, power and exponential functions. Furthermore, a numerical routine is developed during the last step of the SSM, where the shift factors are computed taking into account the rescaling and the dwell times of each level of stresses. The processing of the SSM raw data has revealed that the rescaling parameters are the most determining factors to reach an accurate long-term creep curves. The rescaling process has shown an appropriate time, whether achieved by the exponential or power functions. Larger shift factors for exponential functions are assessed and therefore a long period of creep master curve was obtained.

**KEYWORDS.** Creep; Polyamide 6; Fitting function; SSM method; Master curve.



**Citation:** Tedjini, M., Sedira, L., Guerira, B., Meftah, K., On the use of the stepped isostress method in the prediction of creep behavior of polyamide 6, *Frattura ed Integrità Strutturale*, 62 (2022) 336-348.

**Received:** 13.07.2022

**Accepted:** 20.08.2022

**Online first:** 01.09.2022

**Published:** 01.10.2022

**Copyright:** © 2022 This is an open access article under the terms of the CC-BY 4.0, which permits unrestricted use, distribution, and reproduction in any medium, provided the original author and source are credited.



## INTRODUCTION

All mechanical structures are subjected to instantaneous loads which cause either elastic, plastic or combined behaviors. Nevertheless, a viscous effect under monotonic loads can be observed under different scenarios, the most common being dependence on the rate of deformation, dependence on temperature, creep and relaxation [1]. Although it is generally overlooked for some solid materials, the viscous effects play a major part in defining the mechanical response of polymers.

Many experiments were conducted with different techniques to predict the mechanical behavior of materials, starting with simple mechanical experiments such as tensile [2], compression [3], finishing by creep and relaxation tests [4]. However, the creep was among the most important natural phenomena which can describe the material behavior overtime just under his weight influence and through that, we can find further mechanical properties.

Thus, the creep test is conducted on material in order to measure its tendency to deform under constant loading; however, this test requires a very long dwell time [5]. Formerly, the heat factor was considered as the main accelerator of the creep behavior with very large scale time. It is assumed that the creep response for one temperature can be achieved by another temperature at delayed time, the Time-Temperature Superposition Principle (TTSP) was therefore developed and given serious results [6-8]. However, since the elevated temperature may affect the chemical properties of the tested material, a particular care should be devoted to TTSP when the thermo-sensitive materials are processed.

To avoid the negative temperature effect and following an equivalent energy loading, the high stress level is also considered as a creep accelerator factor. Therefore, the Time Stress Superposition Principle (TSSP) was derived from the TTSP and adopted in several researches where improved results are obtained [9,10]. Among others, Hadid et al. [9] have used this approach to predict the long-term material creep behavior of the injection fiber glass reinforced polyamide, an improved empirical model (power law) is used and an excellent superposition of curves is obtained. Based on both temperature and stress effects, a novel approach called Time Temperature Stress Superposition concept (TTSS) is invented thereafter to reduce abundance of samples and to get more accurate results [11,12]. This last one remains very complex, even though it overcomes the negative heat impact and the samples abundance.

Dealing with temperature loads as piecewise constant functions is considered afterwards as a revolution in the long term prediction techniques. Therefore, the Stepped Isothermal Method (SIM) [13] was developed firstly by Thornton et al. [14] and successfully used in several subsequent researches. This approach helped to reduce the large number of samples; but it maximizes the heat impact possibility. When dealing with thick specimens, concern regarding the rapid heating and the non-uniform temperature distribution in the specimen needs to be investigated [15].

As logical extension of SIM method, the technique of Stepped iso-Stress Method (SSM) is emerged as an enhanced solution to both problems: the multiplicity of samples and the heat effect. Recent studies have been performed by Giannopoulos et al. [16,17] that have dealt with Kevlar material and Aramid yarns in terms of mechanical properties, creep, stress and rupture. After that, the effectiveness of this method versus the TSSP method, for specimens of polyamide 6 having a large thickness, has been confirmed in co-author's previous work [5]. As a sequel to this work, the authors [15] analyzed the effect of different testing parameters of the SSM on a commercial polyamide 6 creep tests. The obtained master curves based on power law in rescaling process, correlate well with those obtained with the classical TSSP. The authors have shown that the variation in the dwell time or the change in the stress increment do not affect the creep of studied material. Later, Tanks et al. [18] applied two numerical processing in the SSM method in order to investigate the creep behavior of unidirectional carbon lamina used in rehabilitating prestressed concrete structures. Both of power-law and Prony series methods are used in rescaling procedure for addressing stress history. The power-law was shown to be more conservative by overestimating creep strains, but this is less material efficient for design over the long-term [18]. Recently, Guedes [19] proposed an analytical method to process the SSM raw data. Based on two different viscoelastic models, the method is validated through numerical simulations to assess the creep tests. Also, in order to study the effect of multilayered material on the physico-mechanical properties of bamboo-polypropylene composite (BPCs), Hsu et al. [20] extended their analysis to time depending behavior using the SSM accelerated creep approach. The results have shown that the SSM creep master curves agree well with the long-term experimental creep. The creep master curves were also not influenced by different stress increments and dwelling time variations.

One of the numerical problems encountered with accelerated techniques in construction of the long-term creep curve of plastic materials is uncertainty the fitting method used to address stress or temperature history, which affects the magnitude of the shift factors developed from the data. The uncertainty can be reduced by testing multiple samples but at significant cost. In this context, some convergence problems were raised in our previous works [15], this was due to efficiency of the method used in solving of the optimization problem on one hand, and to the high number of the data



points addressed in fitting process, on the other hand. To this end, the extrapolation model was performed using limited number of points from the starting range of the short-term creep, which did not necessarily lead to a perfect model. An approach that help to overcome this problem consists to use an improved solving method, which is enhanced with additional convergence criterion, can fulfill a good convergence with merely random initial conditions. In order to simulate the creep deformations behavior of the adhesive joints through finite element-based numerical analyses, Sadigh et al. [21] have used the called Levenberg-Marquardt algorithm to fit a power-law model at a variety of stress and temperature levels. The goodness of the fitting procedure was checked using the Standard Error of their estimations.

The main goal of the present study is to investigate the effect of the numerical processing data on the construction of the master creep curves of polyamide 6 using the Stepped isostress Method. Three extrapolating functions are tested during the stress history rescaling and an improved method for solving the optimization problems is used. In addition, a numerical routine is developed in order to estimate the shift factors and to perform all the corresponding time shifting operations. This is expected to achieve improved long-term-creep curves.

## MATERIALS AND METHODS

### *Preparation of Polyamide*

The material tested in the present work is a polyamide 6, trade mark DOMAMID 6BKBL, with a melting temperature  $T_f = 221^\circ\text{C}$  and density  $\rho = 1.1 \text{ g/cm}^3$  (ISO 1183). The raw material was mixed using Thermo Scientific HAAKE PolyLab QC extruder (screw speed 30 rpm and heated zones about  $221^\circ\text{C}$  as an average temperature). Plane sheets of 4 mm thickness were manufactured through a compression molding process: the material was heated to a melt temperature and progressively pressed in a rectangular mold (up to 200 bar). Laboratory hydraulic press (Schwabenthan Polystat 300 S) was used for a total time of 10 minutes (4 minutes for preheating and 6 minutes for compression). CAD and a laser process were carried out to design dumbbell-shape specimens. The dimensions of tensile and creep test specimens are chosen as per ISO 527-2, type 1B, with thickness  $h=4$  (see Fig. 1). The specimens are stored in an atmosphere with 20% of humidity for at least one month.

### *Tensile test*

Uniaxial tensile experiments were performed, using moderately thick specimens of PA6. The tests are conducted by Instron 5969 testing machine equipped with 5kN cell force. The specimens are loaded at ambient temperature ( $25^\circ\text{C}$ ) and 30% of humidity. The load was applied by moving the crosshead of the machine at a specific rate of 1 mm/min (according to ISO 527-1: Plastics-Determination of tensile properties). The deformation is measured with an Advanced Video Extensometer (AVE). The traction test allows determining the linear mechanical properties of the polyamide, and the stress levels which will be considered for creep tests.

### *SSM Method*

The classical approach (TSSP) is generally applied to obtain the creep master curve [15,16,19], using a set of tensile creep tests on at least one specimen per each stress level. To overcome these limitations, the SSM technique is adopted in this work with reduced number of specimens and a valuable gain in time. In this SSM tests, the temperature of  $25^\circ\text{C}$  was set and kept constant throughout a period of the tests. The deformation is measured with a clamp extensometer and the machine is controlled by data acquisition software that allows complex loading sequences to be performed. A starting reference load was initially applied to the specimen (5 MPa), and stair-step loads with five levels are programmed (10, 15, 20, 25, 30 MPa). A dwell time of 2 hours for each load step is considered. The method is generally depending on a set of processes clearly performed in the following sections to reach the final results and to get the adequate master curves.

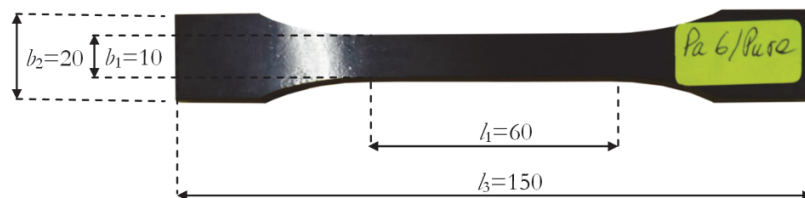


Figure 1: Dimensions of the test specimens.



At the beginning of the experiment, an initial vertical adjustment step is necessary to allow matching of the true starting point for each curve. The change from load to greater level is instantaneous. However, a shift in deformation due to the elastic nature of the material is observed. This step is to erase an element of elasticity and to link the beginning of the current curve with the end of the previous one. In fact, the creep in each step is the accumulation of the creep strain resulting from the applied stress in the current stress level, and also from the creep strain of the previous steps. So, a series of consecutive dependent curves should be separated. However, the creep response of material is considered as a time-invariant behavior since a time-delay on the applied load directly equates to a time-delay of the output response. This aimed at seeking a rescaling time which physically reflects a loading start point, assuming that the test has been conducted under the same stress but on a previously unstressed specimen. According to the time-temperature superposition principle (TTSP), this preprocessing is essential to fulfill the unified conditions of Boltzmann principle.

In order to calculate the rescaling factors, an exponential function is proposed to extrapolate the experimental curves of the raw short time creep, Eqn.1.

$$\varepsilon = \varepsilon_0 + A_1 \exp(-t/t_1) + A_2 \exp(-t/t_2) \quad (1)$$

Where  $t$  is an independent variable.  $\varepsilon_0$ ,  $A_1$ ,  $A_2$ ,  $t_1$  and  $t_2$  are constants. That can be computed by matching with the experiment data through a nonlinear regression for each stress level.

Two others fitting functions are also analyzed. The third degree polynomial function proposed by Achereiner et al. [13], given in Eqn.2 and the power law function presented in our previous research [15], Eqn.3.

$$\varepsilon = \varepsilon_0 + a_1 \cdot t + a_2 \cdot t^2 + a_3 \cdot t^3 \quad (2)$$

$$\varepsilon = \varepsilon_0 \cdot (t - t_0)^n \quad (3)$$

where the constants  $a_1$ ,  $a_2$ ,  $a_3$ ,  $t_0$  and  $n$  are computed as mentioned above. It should be noted that all functions have been fitted considering the full time range in the extrapolation process. Further details are discussed in subsequent section.

The horizontal shifting is a horizontal displacement of the curves in terms of the logarithmic time. It can be achieved by computing the shifting factor ( $\alpha_\sigma$ ), which is the ratio between the time for a viscoelastic process to proceed at an arbitrary stress and the time for the same process to proceed at a reference stress [16]. The creep strain is defined as:

$$\varepsilon_r(\sigma_r, t) = \varepsilon(\sigma, t / \alpha_\sigma) \quad (4)$$

where  $\varepsilon$  is the strain as a function of stress and time,  $\sigma_r$  is the reference stress,  $\sigma$  is the elevated stress and  $\alpha_\sigma$  is the shift factor.

The independent creep curves can be shifted along the logarithmic time axis to obtain the creep master curve at reference stress. The evolution of the shift factor that expresses the creep rate with the stress can be represented by two models, namely the modified model of Williams-Landel-Ferry given in Eqn. 5, or the Eyring model given in Eqn. 6, [15].

$$\log(\alpha_\sigma) = \frac{C_1 \cdot (\sigma - \sigma_r)}{(C_2 + \sigma - \sigma_r)} \quad (5)$$

where  $C_1$  and  $C_2$  are material constants.

$$\log(\alpha_\sigma) = \log\left(\frac{\dot{\varepsilon}}{\dot{\varepsilon}_r}\right) = \frac{V^*}{2.30 \cdot k \cdot T} (\sigma - \sigma_r) \quad (6)$$

where  $\dot{\varepsilon}$  and  $\dot{\varepsilon}_r$  are the strain rate and a reference strain rate respectively,  $V^*$  is the activation volume,  $k$  is Boltzmann's constant and  $T$  is the absolute temperature.

Eqn. 6 is more suitable for the present case, since the creep temperature is below the glass transition temperature. In addition, polyamide 6 is a semi-crystalline polymer, and it is more appropriate to use the Eyring model [15,16,22].



However, the strain rate is considered as a control factor in the PA6 response and creep behavior. It can be graphically determined for each stress level from the slope of the secondary creep portion of the strain-time curve of the experiment result, Eqn. 7.

$$\dot{\varepsilon} = \Delta\varepsilon/\Delta t \quad (7)$$

Contrary to the method used in previous research, where the strain rate is calculated in a global way and taking into account only two points of the curve, i.e. the total slope of the curve, in this work, an instantaneous strain rate will be considered in computation of the shift factor. For this purpose, the same numerical extrapolation proposed in rescaling process (Eqn.1) will be derived and adopted to calculate the strain creep variation, Eqn. 8.

$$\dot{\varepsilon}(t) = -A_1/t_1 \exp(-t/t_1) - A_2/t_2 \exp(-t/t_2) \quad (8)$$

After that, an average value is then computed over the dwell time for each stress level and substituted in Eqn. 6. Both the rescaling and the logarithmic shifting can be done graphically but it is better to follow a numerical procedure at each stress step. Estimation of shift factor  $\alpha_\sigma$  and t-axis shifted values at each stress level can be obtained following numerical method depicted in Fig. 2.

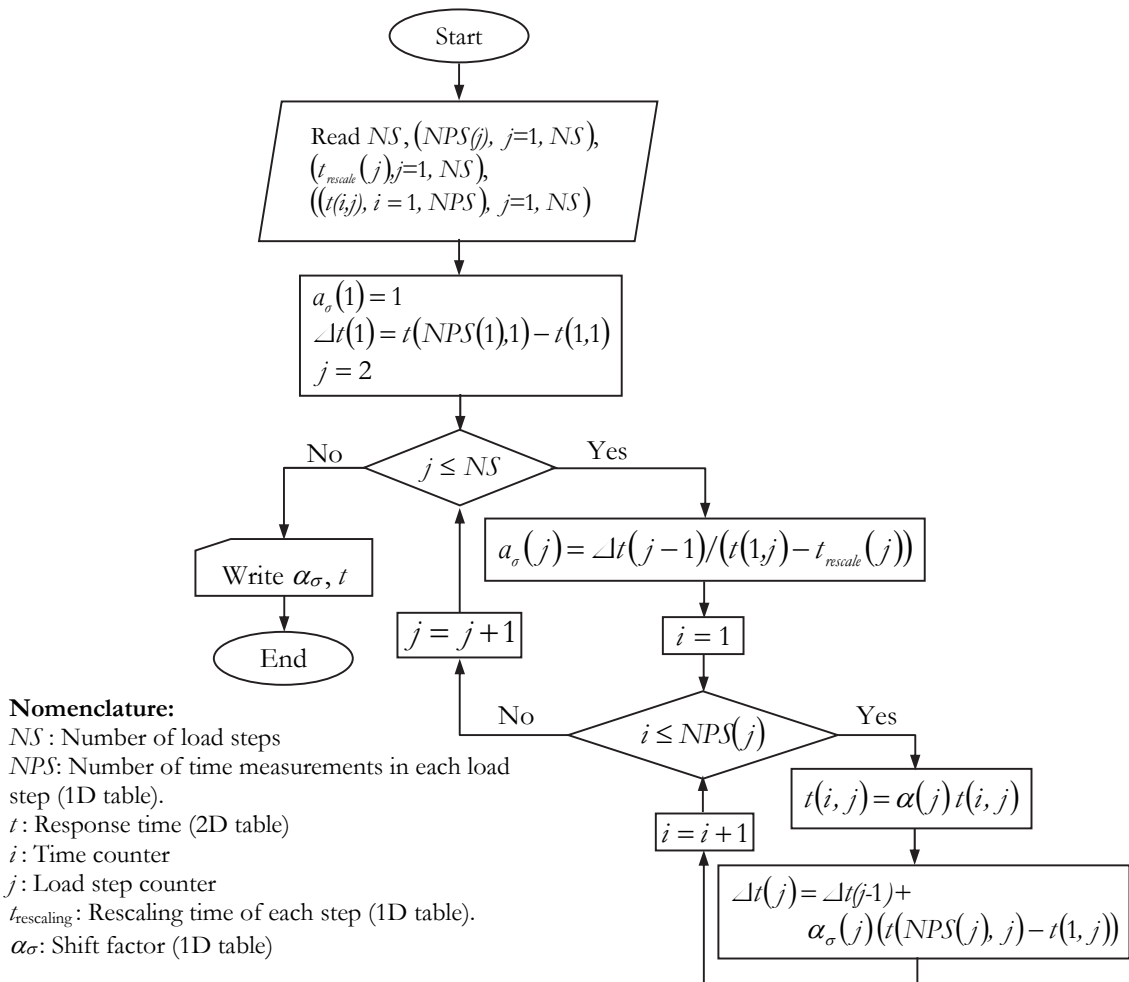


Figure 2: Numerical flowchart of the horizontal shifting.



### Optimization Method

In this research, the constants parameters of the creep strain function are computed using Levenberg-Marquardt method. In fitting  $M(x,t)$ , a function of an independent variable  $t$  and a vector of  $n$  parameters  $x$ , to a set of  $m$  data points  $(t_i, \varepsilon_i)$ , the summation of the weighted squares of the differences between the experimental data  $\varepsilon_i(t_i)$  and the value of the pre-assumed function  $M(x,t_i)$  should be minimized [21], (Eqn. 9). It consists to find the minimum value of the objective function  $F$ , defined as follow:

$$F(x) = \frac{1}{2} \sum_{i=1}^m (f_i(x))^2 = \frac{1}{2} f(x)^T f(x) \quad (9)$$

where  $f_i$  are the residuals for data points  $(t_i, \varepsilon_i)$  defined as:

$$f_i(x) = \varepsilon_i - M(x, t_i) \quad (10)$$

As regards  $F: R^n \mapsto R$ , it follows from the first formulation in Eqn.9, that

$$\frac{\partial F}{\partial x_j}(x) = \sum_{i=1}^m f_i(x)^T \frac{\partial f_i}{\partial x_j}(x) \quad (11)$$

Thus, its gradient is

$$F'(x) = J(x)^T f(x); \quad (J \in R^{m \times n} \text{ is the Jacobian of } f) \quad (12)$$

The non linear least squares problem can be solved by general optimization methods. The Gauss-Newton method is the basic of the very efficient methods, based on a linear approximation to the components of  $f$  (a linear model of  $f$ ) in the neighbourhood of  $x$ : For small  $\|h\|$ , we can write :

$$f(x + h) \approx l(h) \approx f(x) + J(x) h \quad (13)$$

and

$$F(x + h) \approx L(h) \equiv \frac{1}{2} l(h)^T l(h) \quad (14)$$

Full expression of  $L(h)$  can be obtained by substitution (Eqn.13) in (Eqn.14). The gradient and the Hessian of  $L$  are

$$L'(h) = J(x)^T f(x) + J(x)^T h; \quad L''(h) = J(x)^T J(x) \quad (15)$$

So, at a minimum of the sum of squares  $F$ , The Gauss-Newton step  $h$  minimizes  $L(h)$  (i.e.  $L'(h)=0$ ), the unique value can be found by solving

$$(J(x)^T J(x)) h = -g(x); \text{ with } g(x) = -J(x)^T f(x) \quad (16)$$

A damping parameter  $\lambda$  is introduced thereafter by Levenberg and Marquardt [23]. The step  $h_{lm}$  is defined by the following modification to (Eqn.16). However, to ensure a good convergence, i.e. steepest descent direction and reduced step length, the method is controlled by additional stopping criteria, (see Algorithm 1.) where the damping parameter is adjusted at each iteration [24].

$$(J(x)^T J(x) + \lambda I) h_{lm} = -g(x) \quad (17)$$



*Algorithm 1.* Levenberg–Marquardt method [24]

```

begin    $k := 0$  ;  $\nu := 2$  ;  $x := x_0$ 
 $A := J(x)^T J(x)$ ;  $g := J(x)^T f(x)$ 
test: = ( $\|g\| \leq E_1$ ) ;  $\lambda := \tau \times \max\{a_{ii}\}$  ; ( $E_1$ ,  $E_2$  and  $\tau$  are chosen by the user)
while (not test) and ( $k < k_{\max}$ )
   $k := k + 1$ ; Solve ( $A + \lambda I$ )  $h_{lm} = -g$ 
  if  $\|h_{lm}\| \leq E_2 (\|h_{lm}\| + E_2)$  then
    test := true
  else
     $x_{\text{new}} := x + h_{lm}$ 
     $\rho := (F(x) - F(x_{\text{new}})) / \left( \frac{1}{2} h_{lm}^T (\lambda h_{lm} - g) \right)$ 
    if  $\rho > 0$  then
       $x := x_{\text{new}}$ 
       $A := J(x)^T J(x)$ ;  $g := J(x)^T f(x)$ 
      test: = ( $\|g\| \leq E_1$ )
       $\lambda := \lambda \times \max\{1/3, 1 - (2\rho - 1)^3\}$ ;  $\nu := 2$ 
    else
       $\lambda := \lambda \times \nu$  ;  $\nu := 2 \times \nu$ 
  end

```

## RESULTS AND DISCUSSION

### Tensile test

The evolution of the stress with respect to the deformation is presented in Fig. 3. First the material exhibits a linear relationship depicted as Hookean behavior. The slope of the tangent to the stress-strain curve throughout the elastic range is measured (2.9 GPa) and a value of 61 MPa is recorded as a tensile strength at yield elongation (3.40%). The most important in this curve is the elastic limit 37 MPa to use next as a pilot in the creep experience.

### SSM Test

An initial vertical adjustment is performed to the recorded data. All the creep curves are plotted referring to a constant offset ( $\epsilon_0=0.37\%$ ). However, an increase of strain is observed in each stress jump.

In fact, an elastic part which is a real response of the rump function applied in the beginning of each stress is observed between successive stress levels. This elastic strain is measured and eliminated from strain versus time curves of polyamide. Since the elastic modulus is affected after a period of creep, the short term creep curves are adjusted vertically according to the reference [16]. This is achieved graphically by matching every end point of the current strain curve with the start point of the next one, Fig. 4a. So, a series of purely creep curves for each stress level are illustrated in Fig. 4b.

However, in order to take into account the stress history and to perform a master curve, a horizontal rescaling of all curves is carried out through the time-axis. The short-term creep results are dependent responses, that reflect a creep behavior under an accumulate stress. These short term curves are extended to the left in order to seeking the rescaling time ( $t_{\text{resc}}$ ). This is depicted by the required time to achieve the onset of strain ( $\epsilon_0$ ) for the reference stress. For this purpose, the effect of the curve fitting and the extrapolating functions to approximate this time are analyzed using power, third degree polynomial and exponential models. In order to overcome this problem, the already discussed Levenberg–Marquardt method (Algorithm 1) is used in the present work, taking into account the entire database of measurements ( $n \approx 7200$ ). Once the fitting model is aligned to the experimental curve, it is necessary to equalize the expression of the

obtained model and the onset strain  $\varepsilon_0$ . Hence, the requested rescaling time is computed by solving the obtained non linear equation. Associated curves are depicted in Fig. 4c and show an excellent fitting between the three functions and the experimental results.

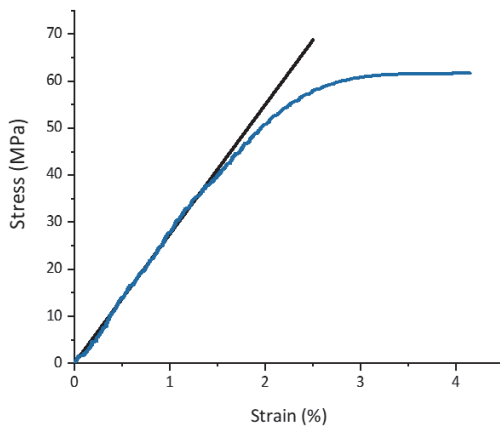


Figure 3: PA6 Tensile curve.

The exponential function fits perfectly the experimental data of the short term curve with  $R^2$  value of 0.999. ( $R^2= 0.976$  and 0.971 for power law and  $R^2=0.997$  for third degree polynomial), for 5 and 10 MPa, respectively.

However, some differences are noted through the extrapolation domain, moving back to the left where the slopes of the functions give rise to a significant deviation, particularly inherent to polynomial function. The rescaling times deduced by each extrapolating functions are reported in Tab. 1. We can see that the results of the power law and exponential function are very close. On the other hand, the polynomial function shows the lowest time, a deviation of up to an hour for high stress levels is occurred. In contrast to some research [18], a greater rescaling time with exponential curve fitting is obtained in the present work. Mathematically, this is in good agreement with the effect of the strain rate, once the strain rate increases, the slope of the curve is systematically high, and therefore, the rescaling time is susceptible to take meaningful values. The most advantageous of the present approach that the total dwelling time range is considered in interpolation process. Unlike to other researches [5,9,16] where only a limited range of time, before and after the onset of each stress/strain response, is considered. On the other hand, all fitting functions are applied so that theirs curves could mimic those of the first creep experimental curve (5 MPa): the curves obtained by the power and exponential functions are in good agreement with data relating to the zero value (expected zero time at  $\varepsilon_0$ ). The first raw of Tab. 1 shows that the power and exponential functions respectively are close to zero value (-20 s and 5.7 s), in contrast with a higher error (-1050 s) assessed by the third polynomial function.

In order to complete the process to obtain the shifting factors, equality between the maximum and the lower strain that can be achieve by the reference and the actual stress respectively is considered. The logarithmic shifting can be done graphically but numerical process depicted in the flow chart is adopted, Fig. 2. Fig. 5a illustrates the computed shifting factors for a set of independent curves obtained by the three extrapolation functions. It can be found that all models give increasing values and the trend of their evolution follows a power function. Fig. 5b refers to a bar chart representation for  $\log(\alpha_\sigma)$ , at first sight, an almost linear variation can be noted. The corresponding values of the power and exponential functions are close to each other and exhibit higher values than the polynomial function.

It is noteworthy that the deviation observed between the shift factors for different functions is justified by the close dependence on the rescaling time. Examining flowchart, Fig. 2, an assumed inversely proportional relationship between the shift factor and the rescaled initial time of each level is found. Each new shift factor is also inversely related to all previous values of rescaling time. The fact that the exponential function has presented the largest rescaling time values, and therefore the shortest time to achieve the maximum strain of the reference level, thus resulting the largest inverse value that affect the shift factors.

The same numerical process is applied to address the shift of the independent creep curves versus t-axis times. The curves for long-term creep prediction in semi-logarithmic and linear time scale are plotted in the Figs. 6a and 6b, respectively. The present method has allowed one to achieve smooth master creep curves without gap between the different short creep responses. On the whole, a large deviation between the three curves was shown in Figs. 7a and 7b. However, all of them reach the same strain with delayed time: the unified master curve for the polynomial function covers a period of



14.27 days approximately ( $t=1.233 \times 10^6$  s). However, a significant improvement can be shown by the power function, where  $t=2.315 \times 10^7$  s, (8.92 months) is obtained. In contrast, a long creep time is estimated at about 2.45 years ( $t=7.624 \times 10^7$  s) using the exponential function.

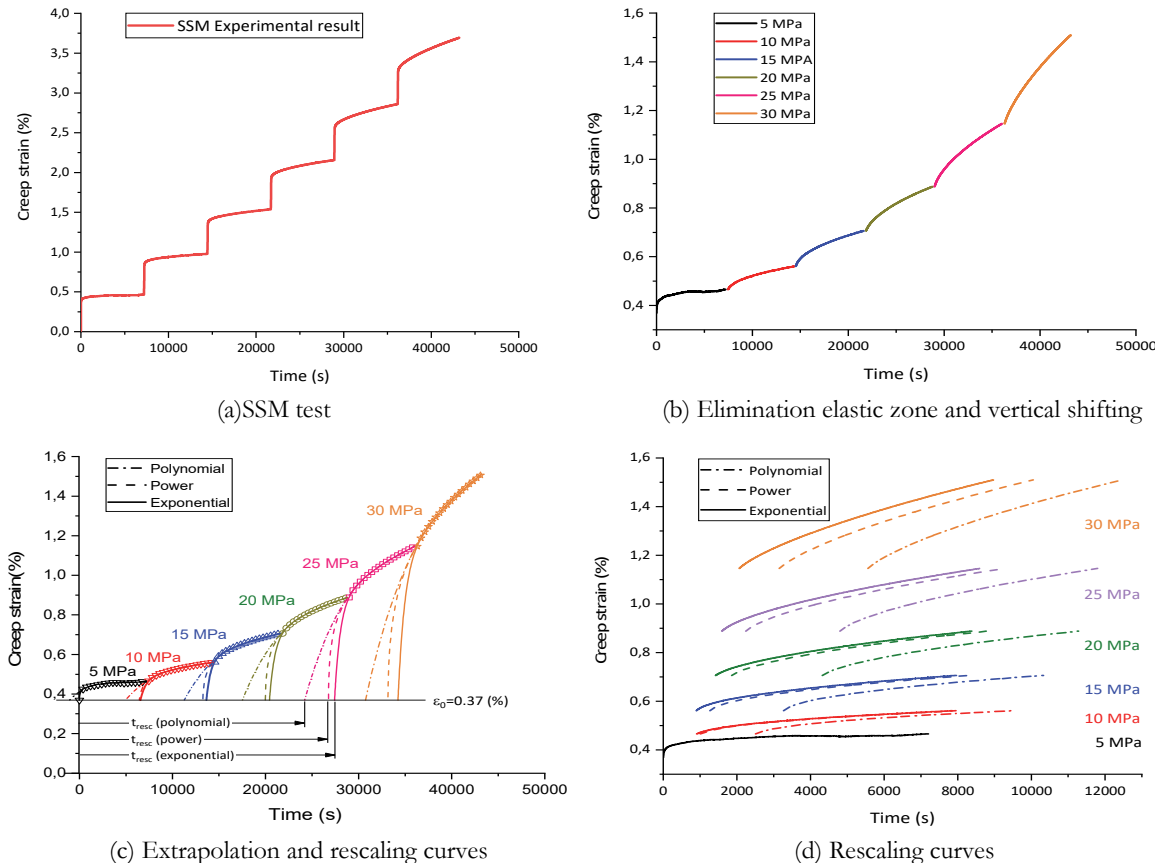


Figure 4: Required handling of the raw data of SSM

Load (MPa)	Rescaling time (h) polynomial	Rescaling time (h) Power law	Rescaling time (h) Exponential
5	-0.2917	0.0016	-0.0056
10	1.3750	1.7914	1.8194
15	3.1306	3.6851	3.7889
20	4.8667	5.5500	5.6722
25	6.7222	7.4322	7.6139
30	8.5389	9.2080	9.5083

Table 1: Rescaling time ( $t_{\text{rescaling}}$ )

This large discrepancy between the third-order polynomial, power law and exponential models can be related to the accuracy of the rescaling time assessment in the beginning of each extrapolation functions. An inadequate value has a significant influence on the horizontal rescaling and shifting processes and affects, therefore the final master curve obtained by each model. However, a numerical criterion that could be helpful to judge the quality of the predictions, assumes that the rheological model of the creep behavior should be operative at all stress level. It found that the third order polynomial is less able to imitate this behavior in the reference stress (Tab. 1). In contrast, the exponential (Prony series approximation) and the power law models that fulfill this assumption, and satisfy the zero time value for zero creep strain, can be considered the better prediction.

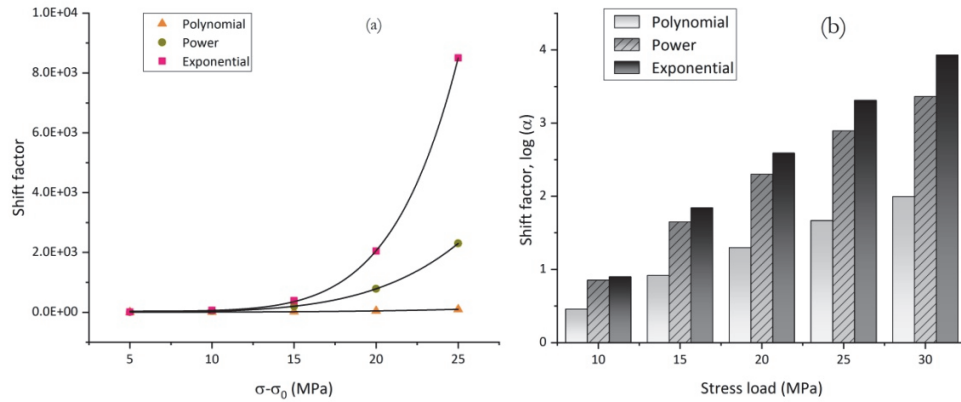


Figure 5: Shift factors values vs. accelerating stresses for different extrapolate functions, (a)  $\alpha_\sigma$  and (b)  $\log(\alpha_\sigma)$ .

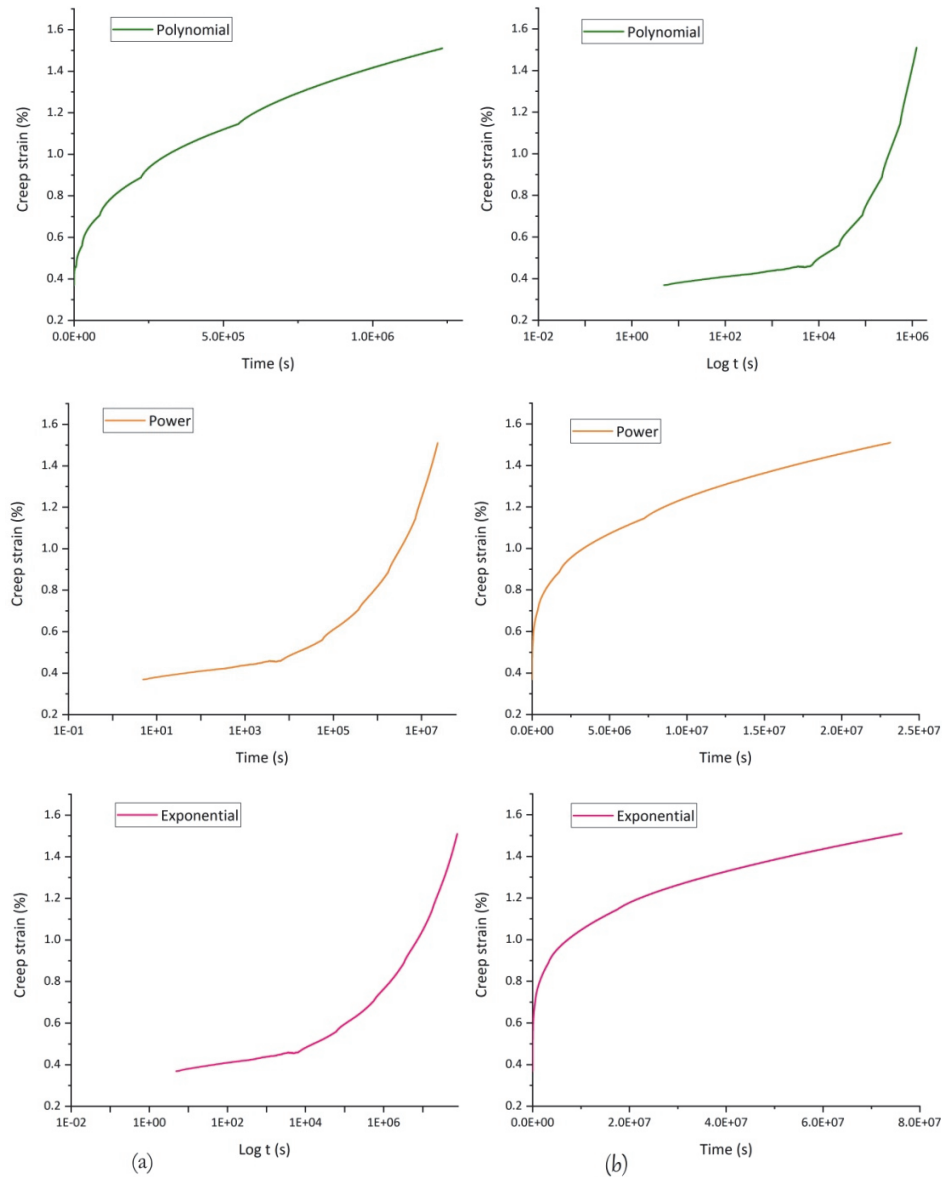


Figure 6: Final master curves with different extrapolate techniques, (a) logarithmic time scale, (b) linear time scale.

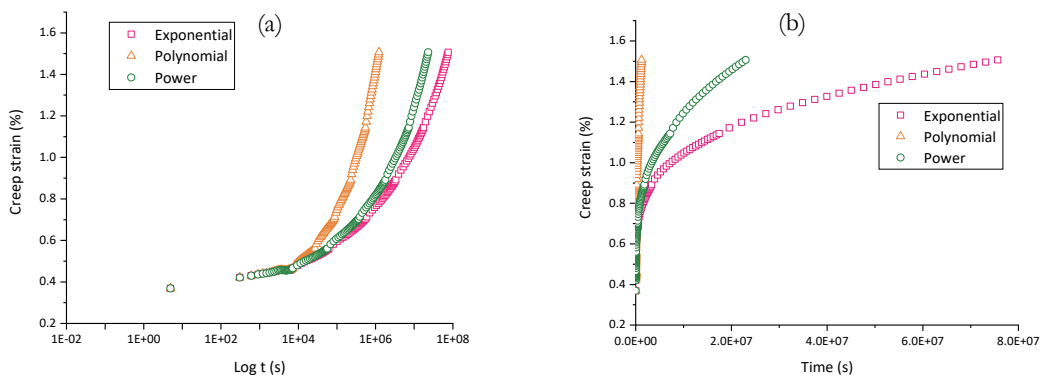


Figure 7: Effect of extrapolation techniques on the prediction of the long term creep, (a) logarithmic time scale, (b) linear time scale.

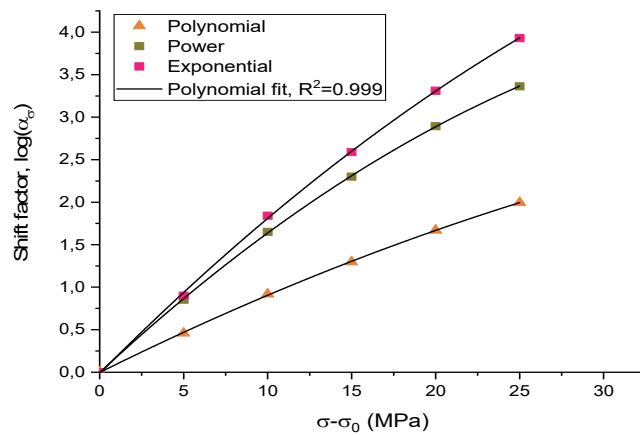


Figure 8: Effect of extrapolation functions on the activation volume

#### *Activation volume*

The activation volume can be presented as the slope between the  $\log(\alpha_\sigma)$  and the accelerator stress variables, Fig. 8. A parabola trends with a coefficient of determination equal to  $R^2=0.999$  have been derived from the different fitting functions using experimental data. However, when assessing the quadratic function, the coefficient of the quadratic term is too small compared to the linear term. Instead, a very close linear form can be addressed with ( $R^2=0.994$ ). It should be noted that, a parabolic form has been adopted by the co-authors [15], which was shown to be more consistent with the Eyring model given in Eqn. 6, and agree well with the previous results, further details are given in [17]. Therefore, the slightly linear variation in the activation volume of each increased stress creates new configuration of molecular chains. The current chain configuration is a build-up of all the previous creep bearings. The fact that the polymer molecules are continuously pulled during the creep process, the creep behavior of a previously strained material occupies a larger activation volume than an unstrained material [15].

## CONCLUSIONS

In the present research, the Stepped Isostress Method is used to predict the long-term creep behavior of moderately thick specimens of polyamide 6. Different empirical model were considered to simulate the strong nonlinearity of the viscoelastic behavior of the considered material under a piecewise constant stress. A third degree polynomial, power and exponential fitting functions are developed and examined trough the construction of the master curve. The assessment of the suggested parameters of the fitted models requires an improved numerical solving method to be considered. The use of Levenberg-Marquardt algorithm allows to overcome the limited use of data points in extrapolation



process and leads to excellent convergence and accuracy. The handling and processing of the SSM raw data have been performed automatically, where a computational subroutine is developed. The numerical process reveals that the magnitude of the shift factor is strongly affected by the accuracy of the inverse of the rescaling time on one hand and has a proportional relationship with the dwell time on the other hand. However, a larger shift factors for the exponential as well as for the power functions are obtained and therefore, larger long-term master curves were estimated with a very close agreement. The construction of the master curve confirms the consistence of the Eyring equation and the relationship between the shift factor and the creep stress.

## ACKNOWLEDGEMENTS

The authors would like to thank the plastics laboratory staff of Biskra cable industry for their help in the preparation of material and specimens.

## REFERENCES

- [1] Dan-Andrei, S. (2016). Viscoplastic behaviour of polyamides. Viscoelastic and viscoplastic materials, IntechOpen.
- [2] Atidel, G., Saintier, N., Dhiab, A., Dammak, F. (2011). Etude du comportement mécanique d'un Polyamide 66 chargé de fibres de verre courtes, *Mec. Ind.*, 12(5), pp. 333–342, DOI: 10.1051/meca/2011104.
- [3] Gnip, I.J., Kersulis, V.I., Vaitkus, S.I., Veyelis, S.A. (2005). Long-term prediction of creep strain of expanded polystyrene, *Mech. Compos. Mater.*, 41(6), pp. 535–540, DOI: 10.1007/s11029-006-0007-6.
- [4] Raghavan, J., Meshii, M. (1998). Creep of Polymer Composites, *Compos. Sci. Technol.*, 57(12), pp. 1673–1688, DOI: 10.1016/S0266-3538(97)00104-8.
- [5] Hadid, M., Guerira, B., Bahri, M., Zouani, K. (2014). The creep master curve construction for the polyamide 6 by the stepped isostress method, *Mater. Res. Innov.*, 18(sup6), pp. s6-336-s6-339, DOI: 10.1179/1432891714Z.0000000001022.
- [6] Yang, J.L., Zhang, Z., Schlarb, A.K., Friedrich, K. (2006). On the characterization of tensile creep resistance of polyamide 66 nanocomposites. Part I. Experimental results and general discussions, *Polymer (Guildf.)*, 47(8), pp. 2791–2801, DOI: 10.1016/j.polymer.2006.02.065.
- [7] Dean, D., Husband, M., Trimmer, M. (1998). Time-temperature-dependent behavior of a substituted poly(paraphenylenes): Tensile, creep, and dynamic mechanical properties in the glassy state, *J. Polym. Sci. Part B Polym. Phys.*, 36(16), pp. 2971–2979, DOI: 10.1002/(SICI)1099-0488(19981130)36:16<2971::AID-POLB12>3.0.CO;2-R.
- [8] Arnold, J.C., Venditti, N.P. (2007). Prediction of the long-term creep behaviour of hydroxyapatite-filled polyethylmethacrylate bone cements, *J. Mater. Sci. Mater. Med.*, 18(9), pp. 1849–1858, DOI: 10.1007/s10856-007-3056-z.
- [9] Hadid, M., Rechak, S., Tati, A. (2004). Long-term bending creep behavior prediction of injection molded composite using stress-time correspondence principle, *Mater. Sci. Eng. A*, 385(1–2), pp. 54–58, DOI: 10.1016/j.msea.2004.04.023.
- [10] Luo, W.B., Wang, C.H., Vu-Khanh, T., Jazouli, S. (2007). Time-stress equivalence: Application to nonlinear creep of polypropylene, *J. Cent. South Univ. Technol. (English Ed.)*, 14(1 suppl.), pp. 310–313, DOI: 10.1007/s11771-007-0271-1.
- [11] Luo, W., Wang, C., Zhao, R. (2007). Application of time-temperature-stress superposition principle to nonlinear creep of poly(methyl methacrylate). *Key Engineering Materials*, 340-341 II, Trans Tech Publ, pp. 1091–6.
- [12] Larbi, S., Berradj, M., Djebbar, A., Bilek, A. (2011). Prediction of Creep Behaviour of the Hybrid Composite Material Using the Accelerated Characterisation Method, *Adv. Mater. Res.*, 324, pp. 356–359, DOI: 10.4028/www.scientific.net/AMR.324.356.
- [13] Achereiner, F., Engelsing, K., Bastian, M., Heidemeyer, P. (2013). Accelerated creep testing of polymers using the stepped isothermal method, *Polym. Test.*, 32(3), pp. 447–454, DOI: 10.1016/j.polymertesting.2013.01.014.
- [14] Thornton, J.S., Allen, S.R., Thomas, R.W., Sandri, D. (1998). The stepped isothermal method for time-temperature superposition and its application to creep data on polyester yarn. *Proceedings of Sixth International Conference on Geosynthetics*, 2, pp. 699–706.



- [15] Hadid, M., Guerira, B., Bahri, M., Zouani, A. (2014). Assessment of the stepped isostress method in the prediction of long term creep of thermoplastics, *Polym. Test.*, 34, pp. 113–119, DOI: 10.1016/j.polymertesting.2014.01.003.
- [16] Giannopoulos, I.P., Burgoynes, C.J. (2011). Prediction of the long-term behaviour of high modulus fibres using the stepped isostress method (SSM), *J. Mater. Sci.*, 46(24), pp. 7660–7671, DOI: 10.1007/s10853-011-5743-x.
- [17] Giannopoulos, I.P., Burgoynes, C.J. (2012). Accelerated and real-time creep and creep-rupture results for aramid fibers, *J. Appl. Polym. Sci.*, 125(5), pp. 3856–3870, DOI: 10.1002/app.36707.
- [18] Tanks, J., Rader, K., Sharp, S., Sakai, T. (2017). Accelerated creep and creep-rupture testing of transverse unidirectional carbon/epoxy lamina based on the stepped isostress method, *Compos. Struct.*, 159, pp. 455–462, DOI: 10.1016/j.compstruct.2016.09.096.
- [19] Guedes, R.M. (2018). A systematic methodology for creep master curve construction using the stepped isostress method (SSM): a numerical assessment, *Mech. Time-Dependent Mater.*, 22(1), pp. 79–93, DOI: 10.1007/s11043-017-9353-0.
- [20] Hsu, C.Y., Yang, T.C., Wu, T.L., Hung, K.C., Wu, J.H. (2018). Effects of a layered structure on the physicomechanical properties and extended creep behavior of bamboo-polypropylene composites (BPCs) determined by the stepped isostress method, *Holzforschung*, 72(7), pp. 589–597, DOI: 10.1515/hf-2017-0165.
- [21] Sadigh, M.A.S., Paygozar, B., da Silva, L.F.M., Tahami, F.V. (2019). Creep deformation simulation of adhesively bonded joints at different temperature levels using a modified power-law model, *Polym. Test.*, 79, DOI: 10.1016/j.polymertesting.2019.106087.
- [22] Ward, I.M., Sweeney, J. (2012). Mechanical properties of solid polymers, John Wiley & Sons.
- [23] Marquardt, D.W. (1963). An Algorithm for Least-Squares Estimation of Nonlinear Parameters, *J. Soc. Ind. Appl. Math.*, 11(2), DOI: 10.1137/0111030.
- [24] Madsen, K., Nielsen, H.B., Tingleff, O. (2004). Methods for non-linear least squares problems. In: Informatics and Mathematical Modelling, T.U. of D., (Ed.), 2 nd Editi, Informatics and Mathematical Modelling, Technical University of Denmark.